

Limiting transport properties of lanthanide and actinide ions in pure water

By E. Mauerhofer, K. Zhernosekov and F. Rösch*

Institute of Nuclear Chemistry, Johannes Gutenberg University Mainz, D-55128 Mainz, Germany

(Received October 29, 2002; accepted in revised form February 5, 2003)

Lanthanides / Actinides / Ion micro-viscosity / Ion mobility / Ionic conductivity / Diffusion coefficient

Summary. The limiting transport properties, *i.e.* the limiting ionic conductivity (λ°) and the limiting diffusion coefficient (D°), of lanthanide and actinide ions at 298.15 K have been calculated by means of the microscopic version of the Stokes–Einstein law involving (i) the effective charge and the ionic radius of the ions and (ii) the ion micro-viscosity, *i.e.* the viscosity of the hydrated water molecules in the vicinity of the ion. The latter quantity was derived from the variation of the dynamic properties of the water molecules in the first hydration shell with the surface charge density of common mono-atomic cations of various charges. The obtained results were found to be consistent with the experimental data given in the literature.

1. Introduction

Thermodynamic properties of trivalent lanthanide and actinide ions, such as the enthalpies and entropies of hydration and the standard partial molar volumes, have been extensively studied during the last decade.

Other thermodynamic quantities such as the limiting transport properties, *i.e.* the limiting ionic conductivity (λ°) or the limiting diffusion coefficient (D°), have not been adequately investigated. However, they are particularly interesting in the context of the understanding of the behavior of lanthanide and actinide ions in solutions. They allow to determine the volume of the aqua ions and the total hydration numbers, *i.e.* the number of water molecules in the primary and secondary hydration shells.

In this paper, a procedure is proposed to calculate the limiting transport properties of lanthanide and actinide ions in pure water at $T = 298.15$ K. The obtained results are compared with the experimental values of various sources.

2. Calculational procedure

The conductivity of an ion in pure water, which is the limiting ionic conductivity, λ° ($\text{m}^2 \text{S eq}^{-1}$), is related to the water

viscosity by the Stokes–Einstein equation [1, 2]:

$$\lambda^\circ = \frac{Fz_i e}{6\pi\eta^\circ r_s}, \quad (1)$$

where F is the Faraday constant ($9.64846 \cdot 10^4 \text{ C mol}^{-1}$), e the elementary charge ($1.6022 \cdot 10^{-19} \text{ C}$), z_i the charge number of the ion, η° the viscosity of water ($\eta^\circ = 8.903 \cdot 10^{-4} \text{ kg m}^{-1} \text{ s}^{-1}$ at 298.15 K) and r_s (m) the Stokes radius or hydrodynamic radius. As the behavior of the limiting ionic conductivity is generally difficult to interpret on the basis of the Stokes radius, the Stokes–Einstein law may be expressed as [3]

$$\lambda^\circ = \frac{Fz_i e}{6\pi\tilde{\eta}_i r_i}, \quad (2)$$

where r_i is the ionic radius (m) and $\tilde{\eta}_i$ ($\text{kg m}^{-1} \text{ s}^{-1}$) the ion micro-viscosity (further denoted by the abbreviation i.m.v.).

According to the Nernst–Einstein relation, the limiting diffusion coefficient of the ion, D° ($\text{m}^2 \text{ s}^{-1}$), is given by analogy to Eq. (2) by

$$D^\circ = \frac{kT}{6\pi\tilde{\eta}_i r_i} \quad (3)$$

with k the Boltzmann constant ($1.3807 \cdot 10^{-23} \text{ JK}^{-1}$) and T the absolute temperature (K).

The i.m.v. reflects the effect of the central ion on the structure of the surrounding water. It is thus related to the dynamic behavior of the water molecules in the first hydration shell of the ion. One might interpret the i.m.v. as the viscosity of the water molecules in the first hydration shell of the ion.

The i.m.v. of common mono-atomic cations may be obtained by means of Eq. (2) using well known experimentally determined λ° -values [4] and the appropriate ionic radii [5] (Table 1). For ions with low charge density (K^+ , Cs^+ , ...), $\tilde{\eta}_i$ is found to be lower than the viscosity of water. This indicates that the structure of the water in the vicinity of the ion (first hydration shell) is more disordered than in the bulk solvent, which explains the abnormally high ionic mobility of these ions. Those ions are generally classified as structure-breakers.

For the ions with a high charge density (Na^+ , Mg^{2+} , Co^{2+} , ...) the i.m.v. is found to be higher than the viscosity

* Author for correspondence (E-mail: frank.roesch@uni-mainz.de).

of water suggesting a gain of orientational order for the water molecules close to the ion. These latter ions are referred to as structure makers.

Consequently, the break-up of the first hydration shell is initiated principally by the molecular reorientation of water molecules. The number of water molecules, Δn , leaving the hydration sphere over a period of time in which the outer bulk water shell (second hydration shell) is renewed, may be related to the i.m.v. by [6]:

$$\Delta n = N (1 - e^{-\eta^\circ/\tilde{\eta}_i}), \quad (4)$$

where N is the number of water molecules in the first hydration shell at the time zero, *i.e.* the coordination number. The number of water molecules remaining in the hydration shell during the exchange process is thus $N^* = N - \Delta n$. It can be seen from Eq. (4) that the relative exchange rate of water molecules between the hydration sphere and the bulk, $\Delta n/N$, is an important quantity for the exchange process.

As shown in Fig. 1, $\Delta n/N$ decreases for increasing values of the surface charge density of the ion $\sigma_i = z_i e / 4\pi r_i^2$ (C m^{-2}) owing to the electrostatic interaction between the ion and the surrounding water molecules. The value of $\Delta n/N$ may be obtained from the following analytical expression:

$$\frac{\Delta n}{N} = a \cdot e^{-b\sigma_i} + c \cdot e^{-d\sigma_i}, \quad (5)$$

where $a = 0.8704$, $b = 1.1453$ ($\text{m}^2 \text{C}^{-1}$), $c = 0.2404$ and $d = 5.5544 \cdot 10^{-2}$ ($\text{m}^2 \text{C}^{-1}$) are numerical parameters obtained from the fit of the data plotted in Fig. 1 by means of Eq. (5). Finally, from Eqs. (4) and (5) the i.m.v. of mono-atomic cations may be expressed as follows

$$\frac{1}{\tilde{\eta}_i} = \frac{2}{\eta^\circ} \text{Arc tanh} \left(\frac{a \cdot e^{-b\sigma_i} + c \cdot e^{-d\sigma_i}}{2 - a \cdot e^{-b\sigma_i} - c \cdot e^{-d\sigma_i}} \right). \quad (6)$$

The expression in brackets in Eq. (6) corresponds to the ratio of the number of water molecules exchanged with the bulk (Δn) to the sum of the water molecules coordinated at the time zero (N) and of the water molecules

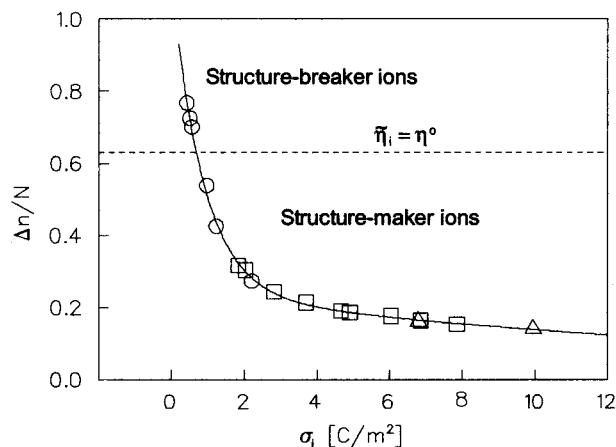


Fig. 1. Relative exchange rate of water molecules between the first hydration sphere and the bulk, $\Delta n/N$, in pure water at 298.15 K versus the surface charge density σ_i of the common mono-atomic ions. The solid line is the fit of the data based on Eq. (5).

translationally immobilized by the ion during the exchange process (N^*).

The values of the i.m.v. and of the limiting ionic conductivity for the common mono-atomic cations calculated by means of Eqs. (6) and (2), respectively, are in good agreement with the experimental values used as initial data for modeling (Table 1).

Thus Eq. (6) in combination with Eqs. (3) or (2) may be used for the determination of the limiting transport properties of cations for which experimental data are missing. This holds in particular for the lanthanide and actinide ions in the valence state +4.

The limiting transport properties of lanthanide and actinide ions were calculated using the corresponding ionic radii and effective charge numbers z_{eff} derived from the analysis of their structural and thermodynamic properties [7] (Tables 2 and 3). The effective charge number z_{eff} is somewhat lower than the formal charge of the ions and reflects the contribution of $4f$ and $5f$ orbitals to the chemical bonding, which might also lead to a certain extent to an affinity of the dynamics of water molecules in the vicinity of the ion.

Table 1. Parameters of hydrated common mono-atomic ions in pure water ($T = 298.15$ K) for the determination of the ion microviscosity of lanthanide and actinide aquo-ions by means of Eq. (6). r_i is the ionic radius, λ° the limiting ionic conductivity and $\tilde{\eta}_i$ the ion microviscosity, Δ the deviation between experimental and calculated data.

Ion	r_i [5] 10^{-10} m	$\lambda^\circ_{\text{exp}}$ [4] 10^{-4} $\text{m}^2 \text{S eq}^{-1}$	$\tilde{\eta}_{\text{exp}}$ Eq. (2) 10^{-4} $\text{kg m}^{-1} \text{s}^{-1}$	$\tilde{\eta}_{\text{cal}}$ Eq. (6) 10^{-4} $\text{kg m}^{-1} \text{s}^{-1}$	$\lambda^\circ_{\text{cal}}$ Eq. (2) 10^{-4} $\text{m}^2 \text{S eq}^{-1}$	Δ %
Cs ⁺	1.74	77.2	6.10	6.01	78.3	1.42
Tl ⁺	1.59	74.7	6.90	6.96	74.2	0.67
K ⁺	1.51	73.5	7.39	7.57	71.8	2.31
Ag ⁺	1.15	61.9	11.52	12.25	58.2	5.98
Na ⁺	1.02	50.0	16.07	15.43	52.1	4.20
Li ⁺	0.76	38.7	27.91	26.86	40.2	3.88
Sr ²⁺	1.18	59.4	23.40	22.73	61.1	2.87
Ca ²⁺	1.12	59.5	24.62	25.00	58.6	1.51
Cd ²⁺	0.95	54.0	31.97	32.49	53.1	1.67
Mn ²⁺	0.83	53.5	36.94	38.12	51.8	3.18
Zn ²⁺	0.74	52.8	41.98	42.30	52.4	0.76
Mg ²⁺	0.72	53.0	42.98	43.26	52.7	0.57
Co ²⁺	0.65	55.0	45.88	46.94	53.8	2.18
Fe ²⁺	0.61	54.0	49.79	49.50	54.3	0.56
Cu ²⁺	0.57	53.6	53.68	52.66	54.6	1.87
Sc ³⁺	0.75	64.7	50.70	49.33	66.5	2.78
Cr ³⁺	0.62	67.0	59.23	59.80	66.4	0.89

3. Results and discussion

Transport properties of the lanthanide ions

The limiting transport properties of lanthanide ions calculated according to Eqs. (2), (3), (6) are summarized in Table 2. Table 2 also gives a comparison of the calculated results to the individual experimental data available in the literature. The variation of λ° - and D° -values of the trivalent lanthanide ions with the atomic number Z is shown in Fig. 2.

The limiting ionic conductivities of trivalent lanthanide ions obtained by Spedding *et al.* [8] from conductance measurements of aqueous solutions of rare earth chlorides at $\text{pH} \approx 6.5$ and $T = 298.15 \text{ K}$ are generally used as reference values. However, as demonstrated by M'Halla and David [9], these values appear to be overestimated since the effect of the hydrolysis of the ions was initially neglected. The hydrolysis phenomenon leads to an increase of the conductivity of the electrolyte solution due to the appearance of hydrogen ions of high mobility in the solution and to a decrease of the ionic strength, affecting thus the relaxation and electrophoretic effects. Taking into account the hydrolysis phenomenon, M'Halla and David [9] found for La^{3+} a λ° -value of $66.4 \pm 0.5 \cdot 10^{-4} \text{ m}^2 \text{ S eq}^{-1}$, which is 5% lower than the value given by Spedding *et al.* [8], $69.7 \text{ cm}^2 \text{ S eq}^{-1}$. This corrected value is in excellent agreement with a recent experimental value, $66.2 \pm 0.5 \cdot 10^{-4} \text{ m}^2 \text{ S eq}^{-1}$, based on independent measurements of the absolute individual ion mobility of La^{3+} at tracer scale in HClO_4 and HNO_3 electrolytes by means of the electromigration technique [10].

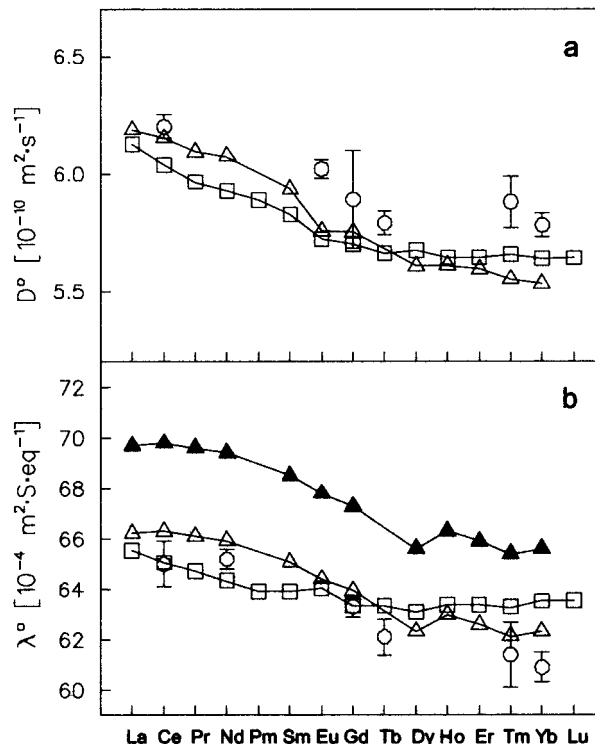


Fig. 2. Limiting transport properties of trivalent lanthanide ions at 298.15 K versus the atomic number Z . (a) limiting diffusion coefficient; (b) limiting ionic conductivity. Calculated data (squares); uncorrected experimental data of Spedding *et al.* [7], (closed triangles), corrected for hydrolysis (open triangles); mean values of other experimental data given in Table 2 (circles).

Table 2. Calculated and experimental limiting transport properties of lanthanide ions ($T = 298.15 \text{ K}$). r_i is the ionic radius, z_{eff} the effective charge of the ion, $\tilde{\eta}_i$ the ion micro-viscosity, λ° the limiting ionic conductivity and D° the limiting diffusion coefficient.

Ion	r_i 10^{-10} m	z_{eff}	$\tilde{\eta}_{i\text{cal}}$ Eq. (6) $10^{-4} \text{ kg m}^{-1} \text{ s}^{-1}$	$\lambda_{\text{cal}}^\circ$ Eq. (2) $10^{-4} \text{ m}^2 \text{ S eq}^{-1}$	$\lambda_{\text{exp}}^\circ$ $10^{-4} \text{ m}^2 \text{ S eq}^{-1}$	D_{cal}° Eq. (3) $10^{-10} \text{ m}^2 \text{ s}^{-1}$	D_{exp}° $10^{-10} \text{ m}^2 \text{ s}^{-1}$
La^{3+}	1.216	2.85	29.32	65.5	69.7 ^a 66.4(5) ^b 66.2(5) ^c	6.12	—
Ce^{3+}	1.196	2.87	30.24	65.1	69.8 ^a 65.0(9) ^d	6.04	6.20(5) ^e
Pr^{3+}	1.179	2.89	31.05	64.7	69.6 ^a	5.96	—
Nd^{3+}	1.163	2.89	31.67	64.3	69.4 ^a 65.2(4) ^d	5.93	—
Pm^{3+}	1.144	2.89	32.41	63.9	—	5.89	—
Sm^{3+}	1.133	2.92	33.07	63.9	68.5 ^a	5.83	—
Eu^{3+}	1.113	2.98	34.29	64.0	67.8 ^a	5.72	6.02(4) ^e
Gd^{3+}	1.069	2.96	35.84	63.3	67.3 ^a 63.3(4) ^d	5.70	5.74(5) ^e 6.04(5) ^f
Tb^{3+}	1.042	2.98	37.02	63.3	62.1(7) ^d	5.66	5.79(5) ^e
Dy^{3+}	1.027	2.96	37.46	63.1	65.6 ^a	5.67	—
Ho^{3+}	1.019	2.99	37.97	63.4	66.3 ^a	5.64	—
Er^{3+}	1.006	2.99	38.46	63.4	65.9 ^a	5.64	—
Tm^{3+}	0.992	3.00	38.93	63.3	65.4 ^a 61(1) ^d	5.65	5.80(5) ^e 5.96(5) ^f
Yb^{3+}	0.984	3.00	39.35	63.5	65.6 ^a 60.9(6)	5.64	5.78(5) ^e
Lu^{3+}	0.977	3.00	39.62	63.6	—	5.64	—
Ce^{4+}	1.149	3.74	37.69	70.9	—	5.05	—

a: from conductance data neglecting effect of hydrolysis [8];

b: data corrected for hydrolysis [9];

c: data from electromigration measurements in free electrolyte [10];

d: data from relative electromigration measurements to Eu^{3+} (paper electrophoresis) [11], with $\lambda^\circ(\text{Eu}^{3+}) = 64.0 \times 10^{-4} \text{ m}^2 \text{ S eq}^{-1}$;

e,f: data determined by open-end-capillary method [12, 13].

Table 3. Calculated and experimental limiting transport properties of actinide ions ($T = 298.15$ K). r_i is the ionic radius, z_{eff} the effective charge of the ion, $\tilde{\eta}_i$ the ion micro-viscosity, λ° the limiting ionic conductivity and D° the limiting diffusion coefficient.

Ion	r_i 10^{-10} m	z_{eff}	$\tilde{\eta}_{i,\text{cal}}$ Eq. (6) 10^{-4} kg m $^{-1}$ s $^{-1}$	$\lambda_{\text{cal}}^\circ$ Eq. (2) 10^{-4} m 2 S eq $^{-1}$	$\lambda_{\text{exp}}^\circ$ 10^{-4} m 2 S eq $^{-1}$	D_{cal}° Eq. (3) 10^{-10} m 2 s $^{-1}$	D_{exp}° 10^{-10} m 2 s $^{-1}$
Ac $^{3+}$	1.330	2.82	25.00	69.5	—	6.57	—
Th $^{3+}$	1.290	2.84	26.53	68.0	—	6.38	—
Pa $^{3+}$	1.275	2.85	27.15	67.5	—	6.31	—
U $^{3+}$	1.226	2.87	29.10	66.0	—	6.12	—
Np $^{3+}$	1.206	2.88	29.94	65.4	—	6.05	—
Pu $^{3+}$	1.187	2.90	30.82	65.0	—	5.97	—
Am $^{3+}$	1.169	2.91	31.59	64.6	64(1) ^a 67(3) ^b 66(—) ^c 71(1) ^d	5.91	6.25(3) ^f 6.19(5) ^g
Cm $^{3+}$	1.154	2.92	32.25	64.3	64(3) ^b	5.87	6.12(6) ^f 6.00(5) ^h
Bk $^{3+}$	1.128	2.93	33.34	63.9	—	5.81	5.95(5) ⁱ
Cf $^{3+}$	1.091	2.95	34.92	63.5	64(3) ^a 59(3) ^b	5.73	5.87(4) ^f 6.17(5) ^g
Es $^{3+}$	1.058	2.96	36.27	63.2	59(3) ^b	5.69	5.77(5) ^f 6.17(5) ^g
Fm $^{3+}$	1.041	2.97	36.99	63.2	58(3) ^b	5.67	—
Md $^{3+}$	1.028	2.98	37.56	63.3	60(3) ^b	5.65	—
No $^{3+}$	1.017	2.99	38.04	63.4	—	5.64	—
Lr $^{3+}$	1.010	3.00	38.37	63.5	—	5.63	—
Th $^{4+}$	1.235	3.50	33.26	69.9	68(1) ^e 69(1) ^e	5.32	—
U $^{4+}$	1.128	3.87	39.01	72.1	68(1) ^e	4.96	—
Np $^{4+}$	1.102	3.91	40.06	72.6	—	4.95	—
Pu $^{4+}$	1.074	4.00	41.39	73.8	—	4.91	—

a: data from conductivity measurements [14];

b,c: data from electromigration measurements (paper electrophoresis) [15, 16];

d: data from electromigration measurements in free electrolyte [17];

e: data from conductivity measurements [21];

f,g,h,i: data determined by open-end-capillary method [12, 18–20].

The λ° -value of La $^{3+}$ calculated in the present work, $65.5 \pm 1.3 \cdot 10^{-4}$ m 2 S eq $^{-1}$, is in good agreement with the latter experimental values. Interestingly, the λ° -values calculated for Ce $^{3+}$, Nd $^{3+}$, Gd $^{3+}$, Tb $^{3+}$, Tm $^{3+}$ and Yb $^{3+}$ agree well with the more recent experimental data deduced from the measurement of the electromigration velocities of the ions relative to Eu $^{3+}$ [11], keeping the calculated λ° -value, $64.0 \pm 1.3 \cdot 10^{-4}$ m 2 S eq $^{-1}$, for Eu $^{3+}$ (circles in Fig. 2b).

Adopting a general reduction of 5% of the initial values of Spedding *et al.* [8] (triangles in Fig. 2b), the λ° -values calculated for the other trivalent lanthanide ions (squares in Fig. 2b) are close to the corrected experimental values.

The calculated diffusion coefficients of the trivalent lanthanide ions (squares in Fig. 2a) are close to the D° -values obtained from the corrected λ° -values of Spedding *et al.* [8] using the effective charge number of the ions, z_{eff} , in the Nernst–Einstein relation (triangles in Fig. 2a). The D° -values calculated for Ce $^{3+}$, Gd $^{3+}$, Tb $^{3+}$, Tm $^{3+}$ and Yb $^{3+}$ are about 2.6% lower than the mean values of the experimental data (circles in Fig. 2a) determined by the open-end capillary method [12, 13]. The difference observed between the calculated and experimental data is higher than the uncertainty of the experimental data. However, the D° -values calculated for Gd $^{3+}$ and Tm $^{3+}$, 5.70 and $5.65 \cdot 10^{-10}$ m 2 s $^{-1}$ are in better agreement with the experimental data of Fourest *et al.* [12] (5.74 and $5.80 \cdot 10^{-10}$ m 2 s $^{-1}$) than with the data of Ouerfelli *et al.* [13] (6.04 and $5.96 \cdot 10^{-10}$ m 2 s $^{-1}$) respectively.

From our calculated data, we observe a transition in the limiting transport properties of the trivalent lanthanide ions around Eu $^{3+}$, Gd $^{3+}$ and Tb $^{3+}$ which corresponds to the well known change of the first hydration number from 9 to 8 with an increasing atomic number Z along the lanthanide series.

Cerium being the most stable tetravalent element among the lanthanides, the dynamic parameters were only calculated for this element. The limiting ionic conductivity of Ce $^{4+}$ is found to be 9% higher than for Ce $^{3+}$ while the limiting diffusion coefficient is 16% lower.

Transport properties of the actinide ions

The calculated limiting transport properties of actinide ions are compared to individual experimental data in Table 3. The variation of λ° - and D° -values of the trivalent and tetravalent actinide ions with the atomic number Z is shown in Fig. 3.

The experimental λ° -values of Am $^{3+}$ determined by various techniques [14–17] (Table 3) differ largely from each other. The λ° -value calculated for Am $^{3+}$, $64.6 \pm 1.3 \cdot 10^{-4}$ m 2 S eq $^{-1}$, is 5% lower than the mean value of the experimental data, $68 \pm 3 \cdot 10^{-4}$ m 2 S eq $^{-1}$. For Cm $^{3+}$ and Cf $^{3+}$, on the other hand, there is a good agreement between the calculated and the mean value of the experimental data [14, 15]. In the case of Es $^{3+}$, Fm $^{3+}$ and Md $^{3+}$ the calculated values are about 7% higher than the experimental values obtained by paper electrophoresis [15], but both the method under con-

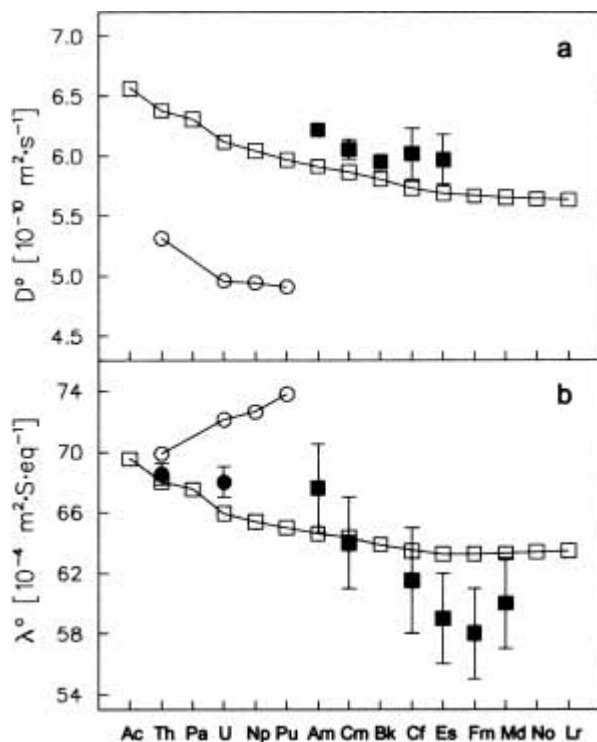


Fig. 3. Limiting transport properties of trivalent (squares) and tetravalent (circles) actinide ions at 298.15 K versus the atomic number Z . (a) limiting diffusion coefficient; (b) limiting ionic conductivity. Calculated data (open symbols); mean values of experimental data listed in Table 3 (closed symbols).

sideration and the difficulty to work on the heavier actinides which are existing only in extremely small concentrations, can explain such a difference.

The calculated limiting diffusion coefficients of Am^{3+} , Cm^{3+} , Cf^{3+} and Es^{3+} are about 4 to 5% lower than the mean values of the experimental data determined by the open-end-capillary method [12, 18–20]. However, the D° -value calculated for Cm^{3+} , $5.87 \cdot 10^{-10} \text{ m}^2 \text{ s}^{-1}$, is in better agreement with the experimental value given by Latrous *et al.* [19], $6.00 \cdot 10^{-10} \text{ m}^2 \text{ s}^{-1}$, than with the value determined by Fourest *et al.* [12], $6.12 \cdot 10^{-10} \text{ m}^2 \text{ s}^{-1}$. In the case of Cf^{3+} and Es^{3+} , the calculated D° -values of 5.73 and $5.69 \cdot 10^{-10} \text{ m}^2 \text{ s}^{-1}$ are on the contrary closer to the experimental values of Fourest *et al.* [12], 5.87 and $5.77 \cdot 10^{-10} \text{ m}^2 \text{ s}^{-1}$. Moreover, using the Nernst–Einstein relation with the appropriate z_{eff} -values, the latter D° -values lead to λ° -values of 65 and $64 \text{ cm}^2 \text{ S eq}^{-1}$ for Cf^{3+} and Es^{3+} . These values are about 9% higher than the experimental values determined in [15]; however, they are close to our calculated data.

From the calculated data, a transition in the limiting transport properties of the trivalent actinide ions is observed around Cm^{3+} , Bk^{3+} and Cf^{3+} . It could also correspond to a change of the first hydration number from 9 to 8 with an increasing atomic number Z along the actinide series, as for the trivalent lanthanide ions.

Since some actinides form stable ions in the tetravalent state, their limiting transport properties were also calculated for this oxidation state.

The limiting ionic conductivity obtained for Th^{4+} , $69.9 \pm 1.4 \cdot 10^{-4} \text{ m}^2 \text{ S eq}^{-1}$, is close to the mean value of the

experimental data, $68.5 \pm 0.7 \cdot 10^{-4} \text{ m}^2 \text{ S eq}^{-1}$, deduced from independent conductivity measurements of aqueous solutions of thorium nitrate and perchlorate salts [21]. The λ° -value found for U^{4+} , $72.1 \pm 1.4 \cdot 10^{-4} \text{ m}^2 \text{ S eq}^{-1}$, appears to be an overestimate with respect to the experimental value, $68 \pm 1 \cdot 10^{-4} \text{ m}^2 \text{ S eq}^{-1}$, obtained from conductivity measurements of aqueous solutions of uranium chloride salts [21]. However, the comparison is limited because of the lack of precise experimental values on the tetravalent actinides.

4. Conclusion

For most of the trivalent lanthanide and actinide ions, the results obtained by calculation are close to the experimental values. However, the limiting transport properties of lanthanide and actinide ions should be remeasured using the modern assortment of analytical techniques in order to check the results of previous experiments. Moreover, independent accurate determination of the limiting diffusion coefficient and of the limiting ionic mobility could lead to an assessment of the effective charge number z_{eff} which is an important parameter in the model used.

The physico-chemical approach developed in this study can thus be interesting to evaluate some thermodynamic data, specially in the case of the heaviest (radioactive) elements, when the typically available number of atoms for experimental studies is very low, *i.e.* insufficient for the application of usual analytical methods.

References

- Stokes, G. G.: *Trans. Cambridge Philos. Soc.* **9**, 8 (1850).
- Einstein, A.: *Ann. Phys.* **17**, 549 (1905).
- Mauerhofer, E., Rösch, F.: *Phys. Chem. Chem. Phys.* **5**, 117 (2003).
- Handbook of Chemistry and Physics*, 78th ed., CRC Press, Boca Ration, FL (1997–1998).
- Shannon, R. D.: *Acta Crystallogr. A* **32**, 751 (1976).
- Impey, R. W., Madden, P. A., McDonald, I. R.: *J. Phys. Chem.* **87**, 5071 (1983).
- David, F., Vokhmin, V., Revel, Fourest, R. B., Hubert, S., Purans, J., Den Auwer, C., Madic, C.: *NRC-5, 5th International Conference on Nuclear and Radio Chemistry*, Pontresina, Switzerland, Sept. (2000) Extended Abstracts, Vol. 1, p. 89.
- Spedding, F. H., Porter, P. E., Wright, J. M.: *J. Am. Chem. Soc.* **74**, 2055 (1952).
- M'Halla, J., David, F.: *Bull. Soc. Chim. Fr.* **4**, 85 (1983).
- Rösch, F., Khalkin, V. A., Milanov, M., Hung, T. K.: *Z. Chem.* **10**, 358 (1987).
- Fourest, B., Duplessis, J., David, F.: *Radiochim. Acta* **46**, 131 (1989).
- Fourest, B., Duplessis, J., David, F.: *Radiochim. Acta* **36**, 191 (1984).
- Ouerfelli, N., Ammar, M., Latrous, H.: *J. Chim. Phys. Phys. Chim. Biol.* **91**, 1786 (1994).
- Fourest, B., Morss, L. R., Blain, G., David, F., M'Halla, J.: *Radiochim. Acta* **69**, 215 (1995).
- Lundqvist, R., Hulet, E. K., Baisden, P. A.: *Acta. Chim. Scand. A* **35**, 651 (1981).
- Fourest, B., David, F., Haltier, E.: *Actinide Res.* **2**, 393 (1988).
- Rösch, F., Khalkin, V. A.: *Radiochim. Acta* **51**, 101 (1990).
- Latrous, H., Oliver, J., Chemla, M.: *Radiochem. Radioanal. Lett.* **53**, 81 (1982).
- Latrous, H., Oliver, J.: *J. Radioanal. Nucl. Chem.* **156**, 291 (1992).
- Latrous, H., Oliver, J.: *J. Mol. Liq.* **81**, 115 (1999).
- Arndt, F., Marx, G.: *Z. Naturforsch.* **36a**, 1019 (1981).